

## EHD Flow Measured by 2D PIV in a Narrow Electrostatic Precipitator with Longitudinal Wire Electrode

**Abstract.** In this paper, results of the electrohydrodynamic (EHD) flow patterns in two narrow ESPs with longitudinally-to-flow wire electrode are presented. The influence of the ESP geometry on the EHD flow generated in the ESP was investigated. The results obtained from 2-dimensional (2D) Particle Image Velocimetry (PIV) showed similarities and differences of the particle flow in the wire-plate and wire-cylinder type ESP.

**Streszczenie.** W niniejszym artykule zaprezentowano wyniki pomiarów struktur przepływu elektrohydrodynamicznego (EHD) wykonanych metodą 2D PIV w dwóch modelach wąskich elektrofiltrów z drutową elektrodą ułotową umieszczoną wzdłuż przepływu. Rezultaty badań wskazują podobieństwa i różnice w strukturach przepływu generowanych w obu typach elektrofiltrów. (Przepływ EHD w wąskim elektrofiltrze z podłużną elektrodą ułotową mierzony przy użyciu metody PIV)

**Keywords:** ESP, electrostatic precipitator, EHD flow, 2D PIV.

**Słowa kluczowe:** elektrofiltr, przepływ elektrohydrodynamiczny, przepływ EHD, 2D PIV.

### Introduction

For decades electrostatic precipitators (ESPs) have been used for dust particles collection, and presently are characterized by a high total particle collection efficiency (up to 99.9%). Therefore, several authors proposed electrostatic precipitation as an alternative control of diesel particulate emission [1-3]. However, there is a problem with submicron particles (i.e. in size range up to  $1.0 \mu\text{m}$ ) [3], which are less electively collected.

The precipitation of particles in the duct of an ESP depends on the dust-particle properties, electric field, space charge, particle physical parameters, electrode geometry and electrohydrodynamic (EHD) secondary flow. The interaction between the electric field and charge and the flow results in considerable turbulences of the flow [4-5], which seems to lower the fine particle collection efficiency. According to some authors [4-5], the turbulence should be reduced to improve the fine particle collection efficiency. Improving other factors, such as ESP electrode geometry or ESP operating conditions, which influence the flow patterns in ESPs, may also increase the fine particle collection efficiency. Data on the flow patterns in ESPs are essential for studying the performance of ESPs.

In this paper results of 2-dimensional (2D) Particle Image Velocimetry (PIV) measurements of the flow patterns in a narrow ESP for two electrode geometries are presented. The PIV measurements were carried out in the observation plane that is perpendicular to the ESP duct.

### Experimental apparatus

The experimental apparatus used in the present work consisted of an ESP, high voltage supply and standard 2D PIV equipment for the measurement of velocity field [6].

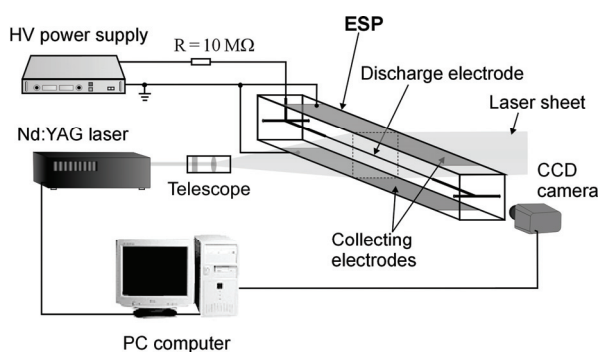


Fig. 1 Experimental set-up

The first ESP used in the present work was a wire-cylinder type. The ESP was a glass cylinder ( $300 \text{ mm} \times 29 \text{ mm}$ , Fig. 2) equipped with a wire discharge electrode and two collecting cylinder-electrodes. A  $0.23 \text{ mm}$  diameter and  $100 \text{ mm}$  long stainless-steel discharge wire electrode was held in the center of the cylinder, parallel to the main flow direction. The collecting electrodes were made of stainless steel cylinder, each with a length of  $100 \text{ mm}$  and inner diameter of  $25.5 \text{ mm}$ .

The second ESP used in the present work was a wire-plate type. The ESP was a narrow glass parallelepiped ( $120 \text{ mm} \times 30 \text{ mm} \times 30 \text{ mm}$ , Fig. 3) equipped with the wire discharge electrode and four collecting plate-electrodes.

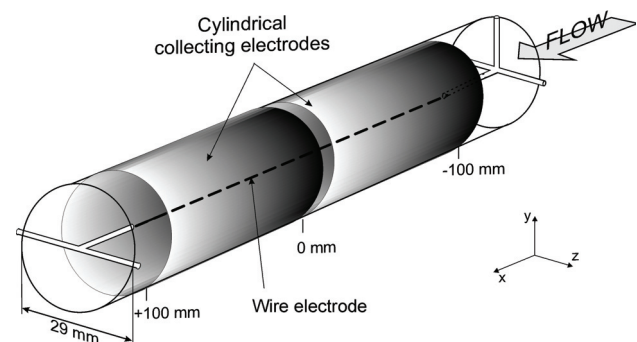


Fig. 2 Wire-cylinder type ESP

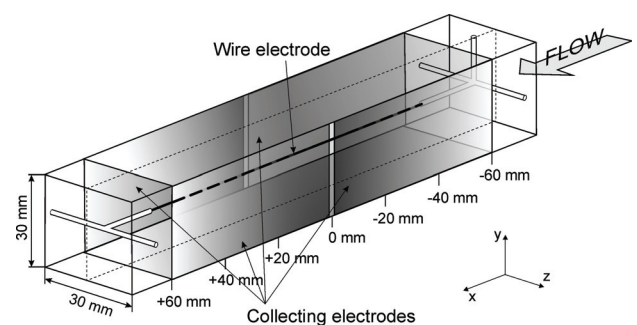


Fig. 3 Wire-plate type ESP

The stainless-steel wire electrode (diameter of  $0.23 \text{ mm}$ , length of  $100 \text{ mm}$ ) was mounted in the middle of the ESP,

parallel to the main flow direction. The collecting electrodes were four plates (120 mm long and 27 mm wide, made of aluminium tape of a thickness of 50  $\mu\text{m}$  glued on dielectric supporting plates) placed on all four walls of the ESP. In both ESPs, positive or negative voltage of 10 kV was supplied to the wire electrode through a 10 M $\Omega$  resistor. Air flow seeded with cigarette smoke was blown along the ESP duct with an average velocity of about 0.9 m/s.

The PIV measurements were carried out in the wire electrode mid-plane (i.e. at  $x = 0$  mm), perpendicularly to the wire and the collecting electrodes. The velocity fields presented in this paper resulted from the averaging of 100 measurements, which means that each velocity map was time-averaged.

## Results

Results of the 2D PIV measurements for both electrode geometries are shown in Figs. 4-7. They show instantaneous image of the dust particles and averaged flow patterns (i.e. flow velocity field and flow streamlines) in the transverse mid-plane (the  $y$ - $z$  plane) of the ESP. At the primary flow average velocity of 0.9 m/s, the Reynolds number was  $Re = 1460$  (for the wire-cylinder type ESP) and  $Re = 1550$  (for the wire-plate type ESP). The Reynolds number was calculated using a formula [7]:

$$(1) \quad Re = \frac{V \cdot L}{\nu}$$

where the primary flow velocity  $V = 0.9$  m/s, characteristic length (plate-plate distance or diameter of the ESP channel)  $L = 0.0255$  m (for the wire-cylinder type ESP) or  $L = 0.027$  m (for the wire-plate type ESP) and air dynamic viscosity  $\nu = 1.57 \times 10^{-5}$  m<sup>2</sup>/s.

Results presented in this paper describe the motion of the dust particles after applying the voltage in the ESP. The patterns measured without applied voltage (not presented in this paper) correspond to the primary flow motion. A slight movement of the dust particles exist in the  $y$ - $z$  plane, the velocity  $y$ - and  $z$ -components are very low (below 0.05 m/s). Due to the voltage applied, a strong secondary flow, caused by the electrohydrodynamic (EHD) forces, is formed in the  $y$ - $z$  plane, i.e. transversely to the flow duct.

It is seen from Figs. 4-7 that due to the EHD forces the dust particles flow from the ESP center (i.e. from the discharge wire electrode) towards the collecting electrodes.

Figs. 4-5 show the results of 2D PIV measurement in the wire-cylinder type ESP.

The flow patterns for the wire-cylinder type ESP show in Fig. 4 are for the positive high voltage. The total discharge current was 140  $\mu\text{A}$ . After applying the high voltage, due to the EHD forces the dust particles are pushed from the wire electrodes outwards by the electric force which is strongest around the wires and move radials towards the cylindrical collecting electrodes with migration velocity up to 0.3 m/s. The dark circular area around the wire electrode seen in Fig. 4a is the area from which the particles have already been removed. The particle flow is very regular (Fig. 4b-c).

The transverse flow patterns in the wire-cylinder type ESP for negative voltage polarity are presented in Fig. 5. The total discharge current was 290  $\mu\text{A}$  (i.e. higher than for positive polarity). At negative polarity, the instantaneous particle flow pattern (Fig. 5a) does not exhibit any regularity as it does just after applying the positive high voltage. The particle flow pattern at negative polarity is irregular and turbulent (Fig. 5b-c).

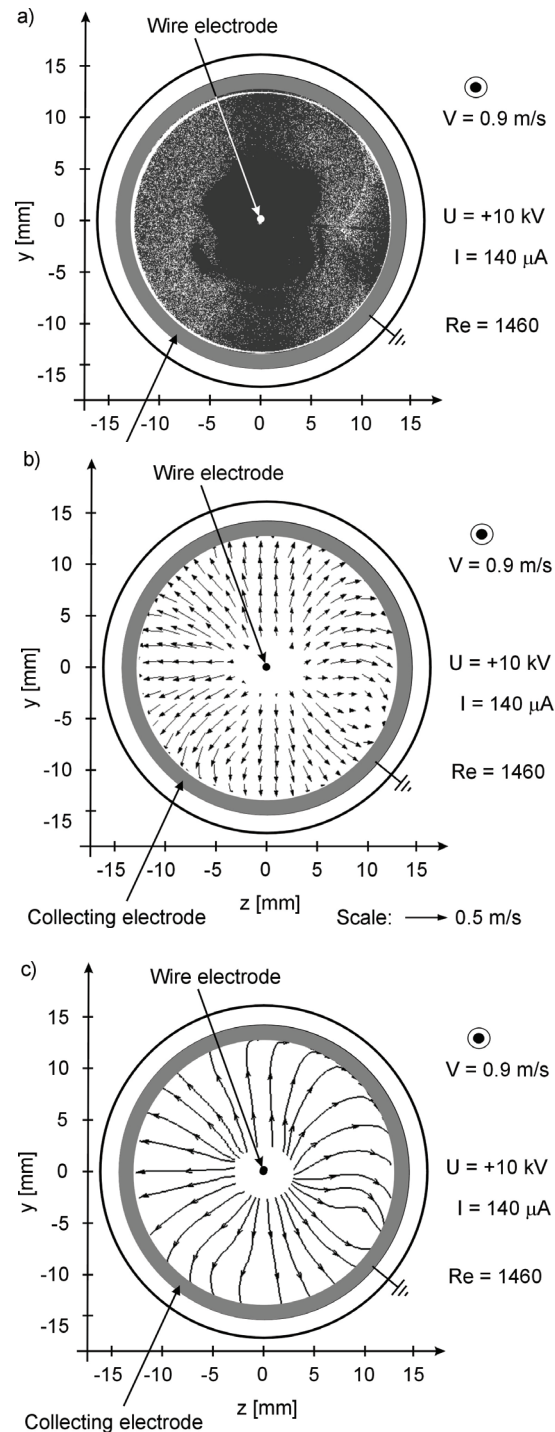


Fig. 4 Instantaneous image of the dust particles (a), averaged flow velocity field (b) and averaged flow streamlines (c) in the wire-cylinder type ESP. Average total discharge current 140  $\mu\text{A}$ . Positive voltage of 10 kV.  $\odot$  - show the direction of the primary flow

The removal of the dust particles from the areas around the electrode wire is faster than in the case of positive polarity. The dust particles migrate with the velocity up to 0.4 m/s in the direction of the collecting electrodes.

Figs. 6-7 show the results of 2D PIV measurement in the wire-plate type ESP.

Results presented in Fig. 6 show the transverse flow patterns in the ESP for the positive polarity. The total discharge current was 200  $\mu\text{A}$ .

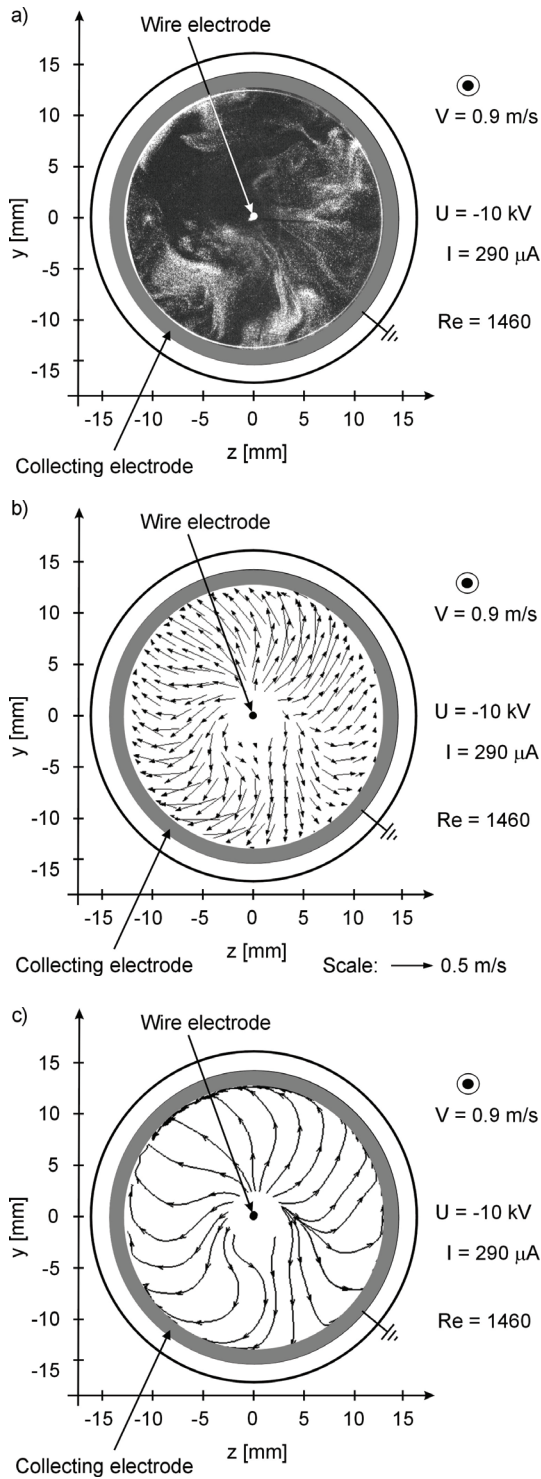


Fig. 5 Instantaneous image of the dust particles (a), averaged flow velocity field (b) and averaged flow streamlines (c) in the wire-cylinder type ESP. Average total discharge current 290  $\mu\text{A}$ . Negative voltage of 10 kV.  $\odot$  - show the direction of the primary flow

In the case of the wire-plate type ESP after applying the positive high voltage the particle flow is more disturbed than in the wire-cylinder type ESP. Four strong streams of the dust particles move towards plate electrodes. After reaching the plate electrode, each of four streams meets two oncoming neighboring streams which results in scattering of the streams. Small double vortex structures are formed in all corners of the ESP cross section. The migration velocity is up to 0.4 m/s, slightly higher than in the wire-cylinder type ESP.

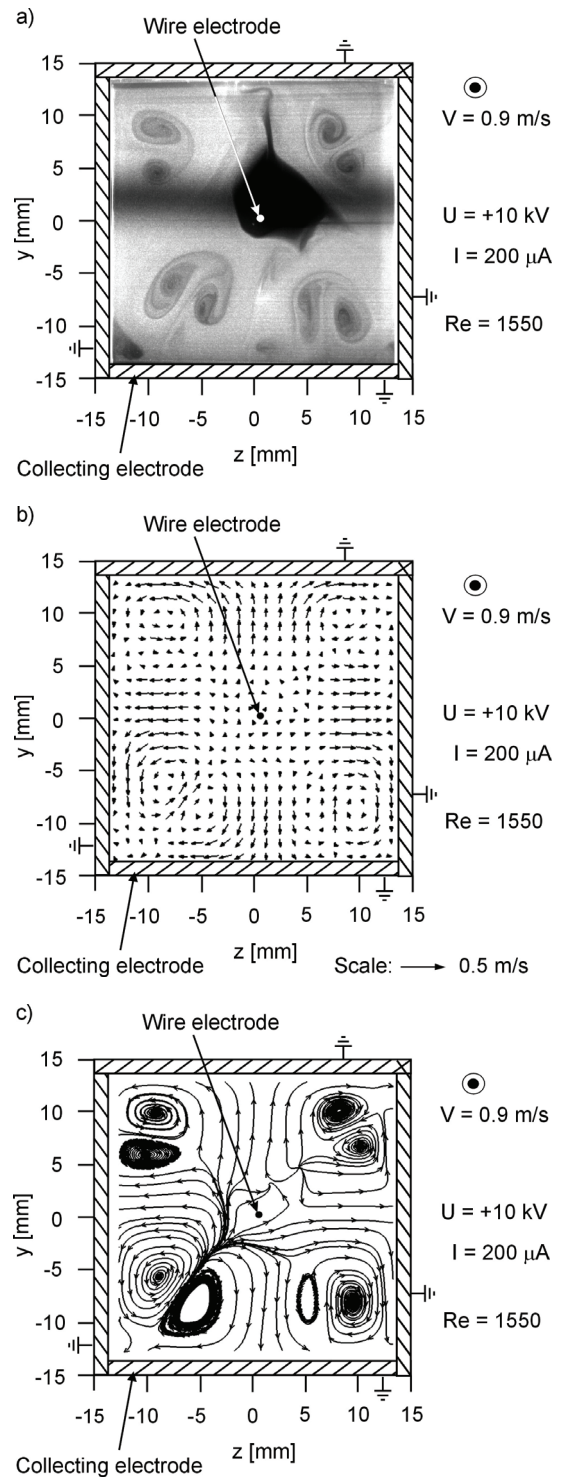


Fig. 6 Instantaneous image of the dust particles (a), averaged flow velocity field (b) and averaged flow streamlines (c) in the wire-plate type ESP. Average total discharge current 200  $\mu\text{A}$ . Positive voltage of 10 kV.  $\odot$  - show the direction of the primary flow

The transverse flow patterns in the wire-plate type ESP for the negative polarity are presented in Fig. 7. The total discharge current was 235  $\mu\text{A}$ .

It is seen from Figs. 7 b and c that the time-averaged flow pattern confirms the features of the particle flow for negative polarity (Figs. 6 b and c). Several small vortex structures were formed in the ESP cross section. However, the instantaneous particle flow is less regular and more turbulent than in the case of positive polarity. The more turbulent character of the flow patterns at negative voltage polarity is probably due to nonuniformity of the negative



corona discharge, which exhibits the form of tufts irregularly distributed along the wire in time and space.

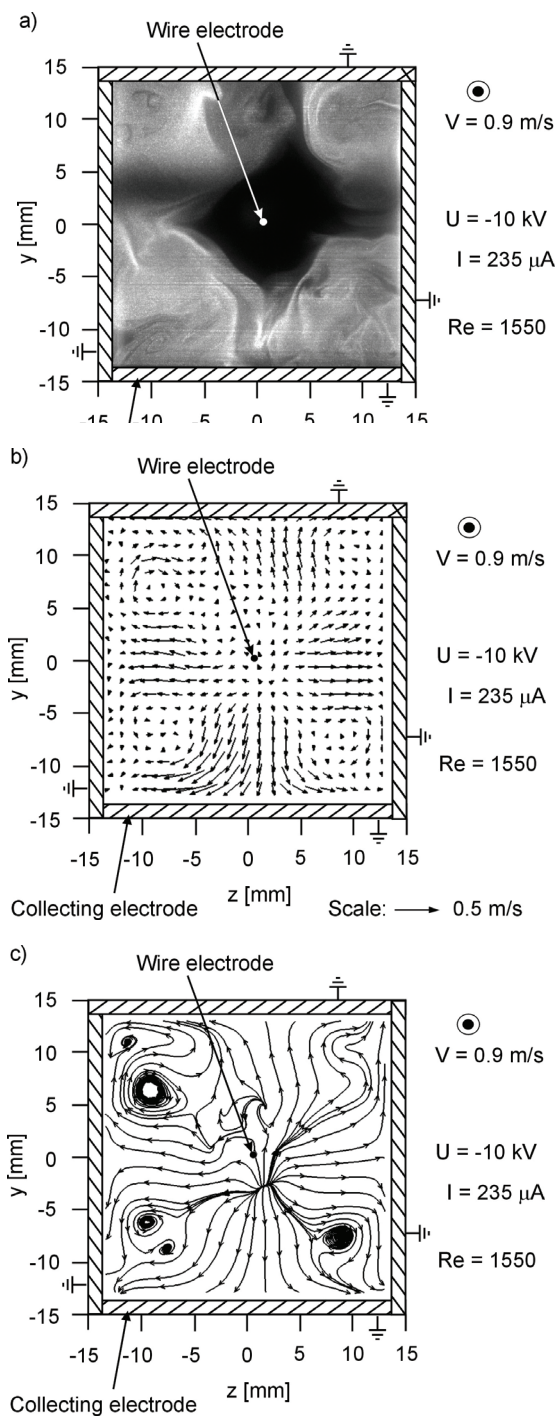


Fig. 7 Instantaneous image of the dust particles (a), averaged flow velocity field (b) and averaged flow streamlines (c) in the wire-plate type ESP. Average total discharge current 235  $\mu\text{A}$ . Negative voltage of 10 kV.  $\odot$  - show the direction of the primary flow

## Conclusions

The presented results of 2D PIV measurements of the particle velocity fields in the narrow ESP showed that the electrode geometry significantly changes the particle flow patterns. Comparing the results for both ESPs one can see, that flow patterns formed by the EHD forces in the plane perpendicular to the main flow are very different. In the wire-plate type ESP vortex structures were formed, while in the wire-cylinder type ESP instead of forming vortices the particle flow was moved radially towards the collecting electrodes.

The different flow patterns, caused by the different collecting electrode geometry, may result in different particle collection efficiency. The particle collection efficiency for both presented electrode geometries are under investigation.

## ACKNOWLEDGMENT

This work was supported by the Ministry of Science and Higher Education (grant PB 281/T02/2010/70, "Iuventus Plus").

## REFERENCES

- [1] Zukeran A., Ikeda Y., Ehara Y., Matsuyama M., Ito T., Takahashi T., Kawakami H., Takamatsu T., Two-Stage-Type Electrostatic Precipitator Re-Entrainment Phenomena Under Diesel Flue Gases" *IEEE Trans. Ind. Appl.*, vol. 35, No. 2, (1999), 346-351
- [2] Saiyasitpanich Ph., Keenera T. C., Khangb S.-J, Lua M., Removal of diesel particulate matter (DPM) in a tubular wet electrostatic precipitator, *J. Electrostatics*, vol. 65, (2007), 618-624
- [3] Kittelson D.B., Reinersen J., Michalski J., Further Studies of Electrostatic Collection and Agglomeration of Diesel Particles, *SAE Paper 910329*, (1991), 145-163
- [4] Atten P., McCluskey F.M.J., Lahjomri A.C., The Electrohydrodynamic Origin of Turbulence in Electrostatic Precipitators, *IEEE Trans. Ind. Appl.* vol. 23, (1987), 705-711
- [5] Yamamoto T., Effects of Turbulence and Electrohydrodynamics on the Performance of Electrostatic Precipitators, *J. Electrostatics*, vol. 22, (1989), 11-22
- [6] Westerweel J., Fundamentals of Digital PIV, *Meas. Sci. Tech.* vol. 8, (1997), 1379-1392
- [7] IEEE-DEIS-EHD Technical Committee, Recommended International Standard For Dimensionless Parameters Used In Electrohydrodynamics, *IEEE Trans. Dielect. Electr. Insul.* 10, (2003), pp. 3-6

**Authors:** M.Sc. Anna Niewulis [aniewulis@imp.gda.pl](mailto:aniewulis@imp.gda.pl) and Dr. Janusz Podliński [janusz@imp.gda.pl](mailto:janusz@imp.gda.pl), M.Sc. Artur Berendt, Centre for Plasma and Laser Engineering, The Szewalski Institute of Fluid Flow Machinery, Polish Academy of Sciences, Fiszerza 14, 80-952 Gdańsk; Prof. Jerzy Mizeraczyk [jmiz@imp.gda.pl](mailto:jmiz@imp.gda.pl), Centre for Plasma and Laser Engineering, The Szewalski Institute of Fluid Flow Machinery, Polish Academy of Sciences, Fiszerza 14, 80-952 Gdańsk and Department of Marine Electronics, Gdynia Maritime University, Morska 81-87, 81-225 Gdynia